Chinese Journal of Natural Medicines

Ten new lignans with anti-inflammatory activities from the leaves of *Illicium dunnianum*

Ting Li, Xiaoqing He, Dabo Pan, Xiaochun Zeng, Siying Zeng, Zhenzhong Wang, Xinsheng Yao, Wei Xiao, Haibo Li, Yang Yu

Citation: Ting Li, Xiaoqing He, Dabo Pan, Xiaochun Zeng, Siying Zeng, Zhenzhong Wang, Xinsheng Yao, Wei Xiao, Haibo Li, Yang Yu, Ten new lignans with anti-inflammatory activities from the leaves of *Illicium dunnianum*, Chinese Journal of Natural Medicines, 2025, 23(8), 990-996. doi: 10.1016/S1875-5364(25)60934-4.

View online: https://doi.org/10.1016/S1875-5364(25)60934-4

Chinese Journal of Natural Medicines 23 (2025) 990-996

Contents lists available at ScienceDirect

Chinese Journal of Natural Medicines

journal homepage: www.cjnmcpu.com/

Original article

Ten new lignans with anti-inflammatory activities from the leaves of *Illicium dunnianum*

Ting Li[a,Δ], Xiaoqing He[a,Δ], Dabo Pan[c], Xiaochun Zeng[a], Siying Zeng[a], Zhenzhong Wang[b], Xinsheng Yao[a], Wei Xiao[b,*], Haibo Li[b,*], Yang Yu[a,*]

[a] *Institute of Traditional Chinese Medicine & Natural Products, College of Pharmacy; State Key Laboratory of Bioactive Molecules and Druggability Assessment; International Cooperative Laboratory of Traditional Chinese Medicine Modernization and Innovative Drug Development of Ministry of Education (MOE) of China; and Guangdong Province Key Laboratory of Pharmacodynamic Constituents of TCM and New Drugs Research, Jinan University, Guangzhou 510632, China*

[b] *State Key Laboratory on Technologies for Chinese Medicine Pharmaceutical Process Control and Intelligent Manufacture, Jiangsu Kanion Pharmaceutical Co., Ltd., Lianyungang 222001, China*

[c] *Department of Medical Technology, Qiandongnan Vocational & Technical College for Nationalities, Kaili 556000, China*

ARTICLE INFO

Article history:
Received 10 October 2024
Revised 13 December 2024
Accepted 19 February 2025
Available online 20 August 2025

Keywords:
Illicium dunnianum
Lignan
Structural elucidation
Anti-inflammatory activity

ABSTRACT

The anti-inflammatory phytochemical investigation of the leaves of *Illicium dunnianum* (*I. dunnianum*) resulted in the isolation of five pairs of new lignans (**1**–**5**), and 7 known analogs (**6**–**12**). The separation of enantiomer mixtures **1**–**5** to **1a**/**1b**–**5a**/**5b** was achieved using a chiral column with acetonitrile–water mixtures as eluents. The planar structures of **1**–**2** were previously undescribed, and the chiral separation and absolute configurations of **3**–**5** were reported for the first time. Their structures were determined through comprehensive spectroscopic data analysis [nuclear magnetic resonance (NMR), high-resolution electrospray ionization mass (HR-ESI-MS), infrared (IR), and ultraviolet (UV)] and quantum chemistry calculations (ECD). The new isolates were evaluated by measuring their inhibitory effect on NO in lipopolysaccharide (LPS)-stimulated BV-2 cells. Compounds **1a**, **3a**, **3b**, and **5a** demonstrated partial inhibition of NO production in a concentration-dependent manner. Western blot and real-time polymerase chain reaction (PCR) assays revealed that **1a** down-regulated the messenger ribonucleic acid (mRNA) levels of tumor necrosis factor α (*TNF-α*), interleukin-6 (*IL-6*), *COX-2*, and *iNOS* and the protein expressions of COX-2 and iNOS. This research provides guidance and evidence for the further development and utilization of *I. dunnianum*.

1. Introduction

Illicium dunnianum (*I. dunnianum*) Tutcher, belonging to the genus *Illicium* of Schisandraceae family, is primarily distributed in Southern China [1]. The roots and rhizomes of this plant have been traditionally utilized as a folk medicine for pain relief, wind dispersion, and rheumatism treatment [2, 3]. Previous phytochemical studies of *I. dunnianum* have identified phenylpropanoids [4–6], flavonoids [7, 8], sesquiterpenes [5, 9], and other chemical components [7, 10]. Modern pharmacological research demonstrates that the extracts of *I. dunnianum* and some of these compounds exhibit multiple biological activities, including anti-inflammation [11], gastrointestinal smooth muscle spasm relief [12], immune regulation [12], and other pharmacological activities [13]. Current studies on the chemical constituents of *I. dunnianum* primarily focus on its roots, stems, and fruits, with limited investigation of its leaves.

Previous research has identified 24 lignans (including nine previously uncharacterized compounds) [14], 15 phenolic acids (including 9 new compounds) [15, 16], two new benzofuran derivatives, and one new *p*-hydroxybenzoate glycoside [16, 17] from the leaves of *I. dunnianum*. In continuing efforts to discover additional bioactive ingredients, 5 pairs of new lignans (**1**–**5**) (Fig. 1), and 7 known analogs (**6**–**12**) were isolated and characterized. The planar structures of **1** and **2** were previously undescribed, and the chiral separation and absolute configurations of **3**–**5** were reported for the first time. Structure elucidation was accomplished through comprehensive spectroscopic data analysis (nuclear magnetic resonance (NMR), high-resolution electrospray ionization mass (HR-ESI-MS), infrared (IR), and ultraviolet (UV)) and quantum chemistry calculations (ECD). The new isolates were evaluated for their inhibitory effect on NO in lipopolysaccharide (LPS)-stimulated BV-2 cells. Compounds **1a**, **3a**, **3b**, and **5a** demonstrated NO production inhibition in a concentration-dependent manner. Western blot and real-time polymerase chain reaction (PCR) assays indicated that **1a** down-regulated the messenger ribonucleic acid (mRNA) levels of tumor necrosis factor α (*TNF-α*), interleukin-6 (*IL-6*), *COX-2*, and *iNOS* and the protein expressions of COX-2 and iNOS. This paper describes the isolation, structural elucidation, and bioactivity assays.

2. Results and discussion

2.1. Structural elucidation of new compounds

Compound **1**, a colorless oil, was isolated as an enantiomeric

* Corresponding author.
E-mail addresses: xw_kanion@163.com (W. Xiao); lihaibo1985124@sina.com (H. Li); 1018yuyang@163.com (Y. Yu)
Δ These authors contributed equally to this work.

https://doi.org/10.1016/S1875-5364(25)60934-4

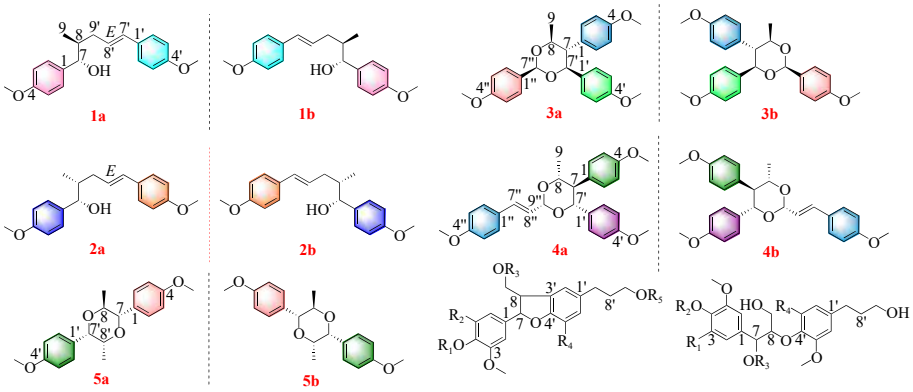

6 $R_3 = R_5 = H$, $R_2 = R_4 = OCH_3$, $R_1 = \beta$-D-Glc (7*S**, 8*R**) **10** $R_2 = R_3 = R_4 = H$, $R_1 = OCH_3$ (7*R**, 8*R**)
7 $R_3 = R_5 = H$, $R_4 = OCH_3$, $R_1 = \beta$-D-Glc (7*S**, 8*R**) **11** $R_1 = R_3 = H$, $R_4 = OCH_3$, $R_2 = \beta$-D-Glc (7*S**, 8*R**)
8 $R_1 = R_2 = R_5 = H$, $R_4 = OCH_3$, $R_3 = \beta$-D-Glc (7*S**, 8*R**) **12** $R_1 = R_2 = H$, $R_4 = OCH_3$, $R_3 = \beta$-D-Glc (7*S**, 8*R**)
9 $R_1 = R_2 = R_3 = H$, $R_4 = OCH_3$, $R_5 = \beta$-D-Glc (7*S**, 8*R**)

Fig. 1 Chemical structures of compounds **1a/1b–12** (red: new compounds).

mixture of **1a** and **1b**. The HR-ESI-MS analysis revealed an ion peak at *m/z* 313.1829 $[M + H]^+$ (Calcd. for 313.1804), corresponding to a molecular formula of $C_{20}H_{24}O_3$. The ^{1}H NMR spectrum (Table 1) demonstrated the presence of two 1,4-disubstituted phenyl rings [δ_H 7.26 (2H, d, *J* = 8.8 Hz, H-2, 6), 7.24 (2H, d, *J* = 8.7 Hz, H-2′, 6′), 6.88 (2H, d, *J* = 8.8 Hz, H-3, 5), 6.83 (2H, *J* =

Table 1 ^{1}H and ^{13}C NMR data for compounds **1a/1b–5a/5b** in $CDCl_3$.

No.	1a/1b		2a/2b		3a/3b		4a/4b		5a/5b	
	δ_C	δ_H (*J* in Hz)	δ_C	δ_H (*J* in Hz)	δ_C	δ_H (*J* in Hz)	δ_C	δ_H (*J* in Hz)	δ_C	δ_H (*J* in Hz)
1	135.8		135.7		130.2		132.0		131.2	
2, 6	127.7	7.26, d (8.8)	128.0	7.25, d (8.8)	129.6	6.92, d (8.7)	128.6	7.94, d (8.6)	128.8	7.32, d (8.7)
3, 5	113.8	6.88, d (8.8)	113.8	6.88, d (8.8)	113.9	6.75, d (8.7)	113.5	6.91, d (8.6)	114.0	6.90, d (8.7)
4	159.0		159.2		158.4		159.1		159.3	
7	77.6	4.54, d (5.1)	78.4	4.43, d (7.5)	55.3	2.71, t (10.3)	55.1	2.68, t (10.3)	85.7	4.26, d (9.0)
8	40.9	1.95	40.7	1.98	78.0	4.25, dq (10.3, 6.2)	77.8	4.16, dq (10.3, 6.1)	67.5	3.78, dq (9.0, 6.3)
9	14.8	0.98, d (6.1)	16.0	0.76, d (6.8)	19.7	1.16, d (6.2)	19.7	1.15, d (6.1)	17.2	0.84, d (6.3)
1′	130.9		130.8		132.2		129.1		129.1	
2′, 6′	127.2	7.24, d (8.7)	127.2	7.29, d (8.7)	128.4	7.05, d (8.8)	129.4	6.89, d (8.1)	132.1	7.74, d (8.7)
3′, 5′	114.0	6.83, d (8.7)	114.1	6.84, d (8.7)	113.4	6.70, d (8.8)	113.9	6.73, d (8.1)	113.5	6.96, d (8.7)
4′	158.8		158.9		158.9		158.5		159.6	
7′	130.7	6.28, d (15.6)	131.0	6.37	84.1	4.85, d (10.3)	84.0	4.75, d (10.3)	77.6	4.52, d (3.4)
8′	126.9	6.02, dt (15.6, 7.0)	126.9	6.11, dd (15.7, 7.9)					74.8	4.34, dq (6.7, 3.4)
9′	37.0	1.95 2.26	36.4	2.14, dtd (13.8, 8.2, 1.3) 2.54, dddd (13.8, 6.6, 4.3, 1.5)					18.1	1.19, d (6.7)
1″					131.4		130.2			
2″, 6″					127.8	7.55, d (8.7)	128.3	7.36, d (8.7)		
3″, 5″					113.7	6.92, d (8.7)	114.0	6.84, d (8.7)		
4″					160.1		159.7			
7″					101.2	5.87	133.3	6.81, d (16.3)		
8″							123.6	6.22, dd (16.3, 5.0)		
9″							101.2	5.52, d (5.0)		
4-OCH_3	55.4	3.89, s	55.5	3.81, s	55.2	3.72, s	55.3	3.72, s	55.2	3.85, s
4′-OCH_3	55.3	3.79, s	55.4	3.80, s	55.2	3.75, s	55.3	3.74, s	55.3	3.81, s
4″-OCH_3					55.4	3.81, s	55.4	3.80, s		

Measured at 600 MHz for ^{1}H and 150 MHz for ^{13}C in $CDCl_3$; multiplets and or overlapped signals are reported without designating multiplicity.

8.7 Hz, H-3′, 5′)], a *trans*-substituted double bond [δ_H 6.28 (1H, t, J = 15.6 Hz, H-7′), 6.02 (1H, dt, J = 15.6, 7.0 Hz, H-8′)], two methines [δ_H 4.54 (1H, d, J = 5.1 Hz, H-7), 1.95 (1H, overlapped, H-8)], one methylene [δ_H 2.26 (1H, m, H_a-9′), 1.95 (1H, overlapped, H_b-9′)], one methyl [δ_H 0.98 (3H, d, J = 6.1 Hz, H_3-9)] and two methoxys [δ_H 3.89 (3H, s, 4-OCH_3), 3.79 (3H, s, 4′-OCH_3)]. The ^{13}C NMR and distortionless enhancement by polarization transfer (DEPT) spectra revealed 20 distinct carbon resonances, comprising 4 quaternary carbons (δ_C 159.0, 158.8, 135.8, 130.9), 12 methines (δ_C 130.7, 127.7 × 2, 127.2 × 2, 126.9, 114.0 × 2, 113.8 × 2, 77.6, 40.9), one methylene (δ_C 37.0) and 3 methyls (δ_C 55.3, 55.4, 14.8). The NMR data suggested that compound **1** was likely a lignan containing two aromatic methoxy substituents, which was subsequently confirmed by ^{1}H–^{1}H correlation spectroscopy (COSY) correlations of H-7/H-8/H_3-9, H-7′/H-8′/H_2-9′, H-8/H_2-9′ and the key heteronuclear multiple bond correlation (HMBC) cross-peaks from H-7 to C-1, C-2, 6; from H-7′ to C-1′, C-2′, 6′; from CH_3O (δ_H 3.89) to C-4 (δ_C 159.0) and from CH_3O (δ_H 3.79) to C-4′ (δ_C 158.8) (Fig. 2). The hydroxy group position at C-7 was determined based on the chemical shift of C-7 (δ_C 77.6) and the molecular formula, thereby establishing the planar structure of compound **1**.

As compounds **1a**/**1b** are classified as 8,9′-neolignans, the relative configurations of C-7 and C-8 were determined through the coupling constant ($J_{7,8}$) of H-7 and the chemical shift of C-7 (*erythro* isomer: $J_{7,8}$ < 5.5 Hz, $\delta_{C\text{-}7}$ < 78; *threo* isomer: $J_{7,8}$ > 6.0 Hz, $\delta_{C\text{-}7}$ > 78), as documented in the literature [18]. The relative configurations of H-7 and H-8 were established as *erythro*-configuration based on the chemical shift of C-7 (δ_C 77.6) and the coupling constant of H-7 ($J_{7,8}$ = 5.1 Hz). Chiral separation yielded enantiomers **1a** and **1b** (Fig. S1), exhibiting mirror image-like ECD spectra (Fig. 3) and opposite optical rotation [**1a**: $[\alpha]_D^{25}$ −35.47 (*c* 0.50, MeOH); **1b**: $[\alpha]_D^{25}$ +39.24 (*c* 0.49, MeOH)]. ECD calculations were conducted for (7*S*,8*S*)- and (7*R*,8*R*)-illiciumligan P using the Gaussian 16 program to determine their absolute configurations. The calculated ECD curve of the (7*S*,8*S*)-configuration matched the experimental ECD spectrum of **1a** (Fig. 3). Therefore, **1a** was definitively identified as (−)-*erythro*-(7*S*,8*S*)-illiciumligan P. As its enantiomer, **1b** was accordingly determined as (+)-*erythro*-(7*R*,8*R*)-illiciumligan P.

Compound **2** (**2a**/**2b**) appeared as a proximate chromatographic peak separated from **1** in RP-HPLC. Both **1** and **2** (*m/z* 313.1839 [M + H]$^+$, Calcd. for $C_{20}H_{25}O_3$, 313.1804) shared the same molecular formula. Comparison of the ^{1}H, ^{13}C, and 2D NMR data between **1** and **2** (Table 1) revealed identical planar structures. The relative configuration of **2** was determined to be *threo* based on the coupling constant of H-7 ($J_{7,8}$ = 7.5 Hz) and the chemical shift of C-7 (δ_C 78.4). Subsequently, **2** was separated into enantiomers **2a** and **2b** through chiral HPLC (Fig. S2). Through comparison of calculated ECD spectra of (7*S*,8*R*)- and (7*R*,8*S*)-illiciumligan Q with the experimental ECD spectra (Fig. 3), **2a** and **2b** were assigned (7*S*,8*R*)- and (7*R*,8*S*)-configurations respectively. Thus, **2a** and **2b** were characterized as (−)-*threo*-(7*S*,8*R*)-illiciumligan Q and (+)-*threo*-(7*R*,8*S*)-illiciumligan Q.

Compound **3** (**3a**/**3b**) was isolated as a colorless oil. Its molecular formula was determined to be $C_{26}H_{28}O_5$ based on HR-ESI-MS analysis at *m/z* 443.1833 [M + Na]$^+$ (Calcd. for 443.1834). The ^{1}H NMR (Table 1) revealed the presence of three 1,4-disubstituted phenyl rings [δ_H 7.55 (2H, d, J = 8.7 Hz, H-2″, 6″), 7.05 (2H, d, J = 8.8 Hz, H-2′, 6′), 6.92 (4H, d, J = 8.7 Hz, H-2, 6, 3″, 5″), 6.75 (2H, d, J = 8.7 Hz, H-3, 5), 6.70 (2H, d, J = 8.8 Hz, H-3′, 5′)], 4 methines [δ_H 5.87 (1H, m, H-7″), 4.85 (1H, d, J = 10.3 Hz, H-7′), 4.25 (1H, dq, J = 10.3, 6.2 Hz, H-8), 2.71 (1H, t, J = 10.3 Hz, H-7)], one methyl [δ_H 1.16 (3H, d, J = 6.2 Hz, H_3-9)] and 3 methoxys [δ_H 3.81 (3H, s, 4″-OCH_3), 3.75 (3H, s, 4′-OCH_3), 3.72 (3H, s, 4-OCH_3)]. The ^{13}C NMR and DEPT spectra displayed 26 carbon resonances, comprising 6 quaternary carbons (δ_C 160.1, 158.9, 158.4, 132.2, 131.4, 130.2), 16 methines (δ_C 129.6 × 2, 128.4 × 2, 127.8 × 2, 113.9 × 2, 113.7 × 2, 113.4 × 2, 101.2, 84.1, 78.0, 55.3) and 4 methyls (δ_C 55.4, 55.2 × 2, 19.7). Analysis of the 2D NMR data indicated that **3** shared an identical planar structure with anemonenorin A [19]. The C-7 and C-8 positions of **3** were confirmed to be part of a ring structure, and the relative configuration was established through nuclear Overhauser effect spectroscopy (NOESY) spectral analysis and coupling constant $J_{7,8}$ values [20, 21]. NOESY correlations between H-7′/H-7″, H7″/H-8, H-7/H_3-9 and coupling constant values of $J_{7,7'}$ = 10.3 Hz and $J_{7,8}$ = 10.3 Hz confirmed the relative configuration, indicating H-7, H-8, H-7′ and H-7″ adopted *β*-, *α*-, *α*- and *α*-orientations, respectively. Compound **3** was subsequently separated into enantiomers **3a** and **3b** using chiral HPLC (Fig. S3). The experimental ECD spectra matched well with the ECD spectra of **3a** and **3b** (Fig. 3). Therefore, **3a** and **3b** were characterized as (+)-(7*S*,8*S*,7′*S*,7″*S*)-anemonenorin A and (−)-(7*R*,8*R*,7′*R*,7″*R*)-anemonenorin A, respectively.

Compound **4** (**4a**/**4b**), isolated as a colorless oil, exhibited a molecular formula of $C_{28}H_{30}O_5$ based on a sodium adduct ion peak (*m/z* 469.1983 [M + Na]$^+$, Calcd. for $C_{28}H_{30}O_5Na^+$, 469.1991) in the positive HR-ESI-MS. Its NMR data (Table 1) revealed signals similar to those of **3**, with an additional *trans*-substituted double bond [δ_H 6.81 (1H, d, J = 16.3 Hz, H-7″), 6.22 (1H, dd, J = 16.3, 5.0 Hz, H-7″)] positioned at C-1″ and C-9″, confirmed by HMBC of H-7″/C-1″, 2″, 6″, 9″ and H-8″/C-1″, 9″ (Fig. 2). Detailed analysis of the 2D NMR data indicated that **4** and illiciumione A [22] shared identical planar structures. The relative configuration of H-7, H-8, H-7′, and H-7″ was established as *α*-, *β*-, *β*-, and

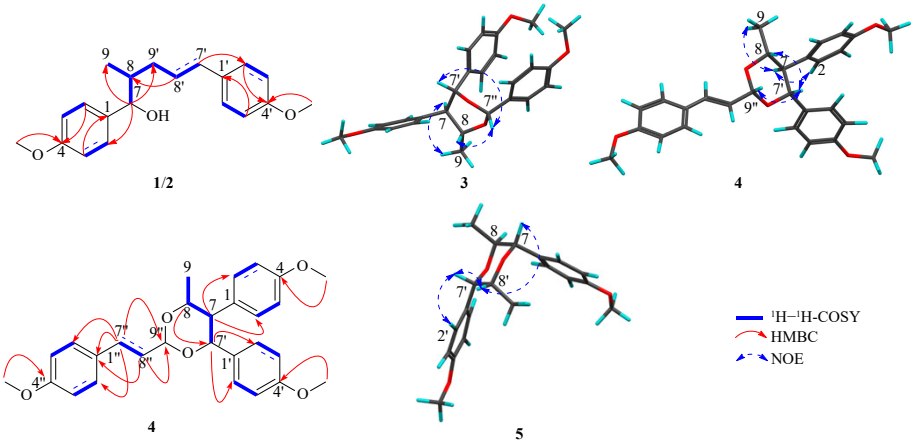

Fig. 2 The key ^{1}H–^{1}H COSY, HMBC correlations of compounds **1**, **2**, and **4**; the NOESY correlations of compounds **3**–**5**.

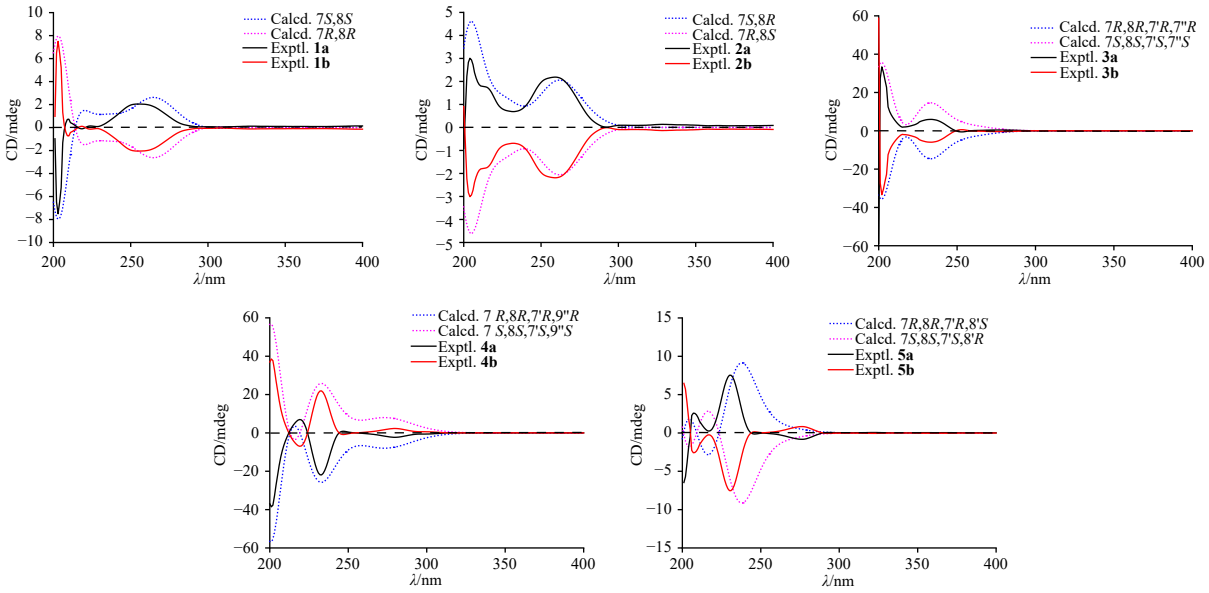

Fig. 3 Calculated and experimental ECD spectra of compounds **1a/1b**–**5a/5b**.

β-orientation using the same methodology as **3**. Subsequent chiral resolution yielded a pair of enantiomers **4a/4b** (Fig. S4) with opposite optical rotations [**4a**: $[\alpha]_D^{25}$ −59.82 (*c* 0.50, MeOH); **4b**: $[\alpha]_D^{25}$ +61.46 (*c* 0.45, MeOH)] and ECD curves. Comparison of experimental and calculated ECD data (Fig. 3) established the absolute configurations of **4a/4b** as (7*R*,8*R*,7′*R*,9″*R*)- and (7*S*,8*S*,7′*S*,9″*S*)-configurations. Thus, **4a** and **4b** were elucidated and designated as (−)-(7*R*,8*R*,7′*R*,9″*R*)-illiciumione A and (+)-(7*S*,8*S*,7′*S*,9″*S*)-illiciumione A, respectively.

Compound **5** (**5a/5b**) was obtained as a colorless oil. Its molecular formula was established as $C_{20}H_{24}O_4$ through analysis of the HR-ESI-MS peak at *m/z* 351.1573 $[M + Na]^+$ (Calcd. for 351.1572). A thorough examination of the NMR data (Table 1) revealed that the planar structure of **5** was identical to verimol H [23]. The relative configurations of **5** were determined as 7,8-*threo*, 7′,8′-*erythro*, based on the NOESY spectrum (Fig. 2) of H-7/H-8′, H-7′/H-2′, 6′ and H-7′/H-8′ and the coupling constant values of $J_{7,8}$ = 9.0 Hz and $J_{7',8'}$ = 3.4 Hz. Subsequent chiral separation yielded a pair of enantiomers **5a/5b** (Fig. S5). Comparison of calculated ECD spectra with experimental ECD spectra (Fig. 3) established their absolute configurations as (7*R*,8*R*,7′*R*,8′*S*)-**5a**, (7*S*,8*S*,7′*S*,8′*R*)-**5b**. Consequently, **5a** and **5b** were identified as (+)-(7*R*,8*R*,7′*R*,8′*S*)-verimol H and (−)-(7*S*,8*S*,7′*S*,8′*R*)-verimol H, respectively.

The seven known compounds (**6**–**12**) were identified as (7*S**,8*R**)-5-methoxydihydrodehy drodiconiferyl alcohol-4-*O*-*β*-D-glucopyranoside [24], (7*S**,8*R**)-urolignoside [24], (7*S**,8*R**)-dihydrodehydrodiconiferyl alcohol-9-*O*-*β*-D-glucopyranoside [25], (7*S**, 8*R**)-dihydrodehydrodiconiferyl alcohol-9′-*O*-*β*-D-glucopyranoside [26], (7*R**,8*R**)-4,7,9,9′-tetrahydroxy-3,5,3′-triethoxy-8-*O*-4′-neolignan [27], (7*R**,8*R**)-7,9,9′-trihydroxy-3,3′,5′-triethoxy-4-*O*-*β*-D-glucosyl-8-*O*-4′-neolignan [28], and rourinoside [29]. The activities of these compounds were discussed in the Supporting information (Tables S2 and S3).

2.2. Anti-inflammatory effects of isolates in LPS-stimulated BV-2 cells

Compounds **1a/1b**–**5a/5b** were evaluated for their inhibitory effects on the production of NO in LPS-induced BV-2 cells. To examine the cytotoxicity of compounds isolated from *I. dunnianum*, MTT assays were performed. The results (Fig. S56) showed that test compounds exhibited no cytotoxicity in BV-2 cells at the testing concentrations. As shown in Fig. 4, compounds **1a**, **3a**, **3b**, and **5a** could partially inhibit NO production in a concentration-dependent manner [hydrocortisone: inhibition rate = 34.5% (10 μmol·L^{-1})]. Meanwhile, the mRNA levels of *TNF-α*, *IL-6*, *COX-2*, and *iNOS* were measured by real-time PCR. As a result, **1a** observably inhibited the mRNA expression in a dose-dependent manner (Fig. 5). Furthermore, we used Western blot to evaluate the inhibitory effects of **1a** on the protein expressions of COX-2 and iNOS. The result showed that **1a** apparently down-regulated the protein expressions of iNOS and COX-2 (Fig. 6) in a dose-dependent manner. The above results demonstrated that **1a** has potential anti-inflammatory activity. In addition, the results revealed that NO inhibitory activities of these compounds is partially correlated with their different configurations. For example, compounds **1a/1b** and **2a/2b** have the same planar structure, and with regard to the anti-inflammatory activity (**1a** > **1b** > **2a/2b**), it suggested that the anti-inflammatory activity of

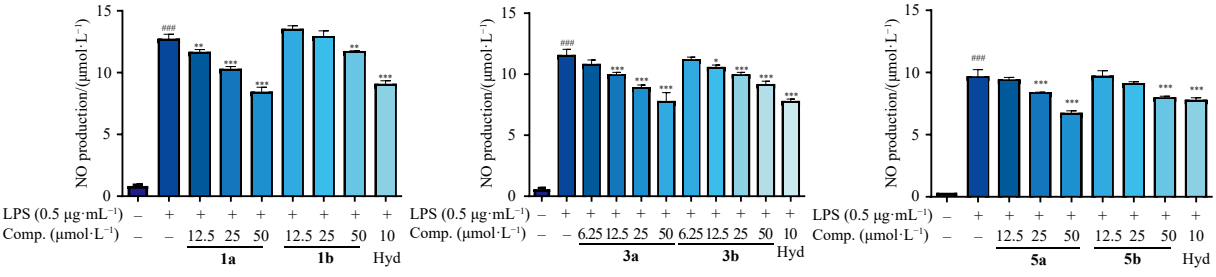

Fig. 4 NO secretion in the supernatant of BV-2 cells from control, LPS, and compounds treated under LPS. The concentrations are presented as mean ± SD (*n* = 3). $^{###}P < 0.001$ *vs* control, $^{*}P < 0.05$, $^{**}P < 0.01$, $^{***}P < 0.001$ *vs* LPS.

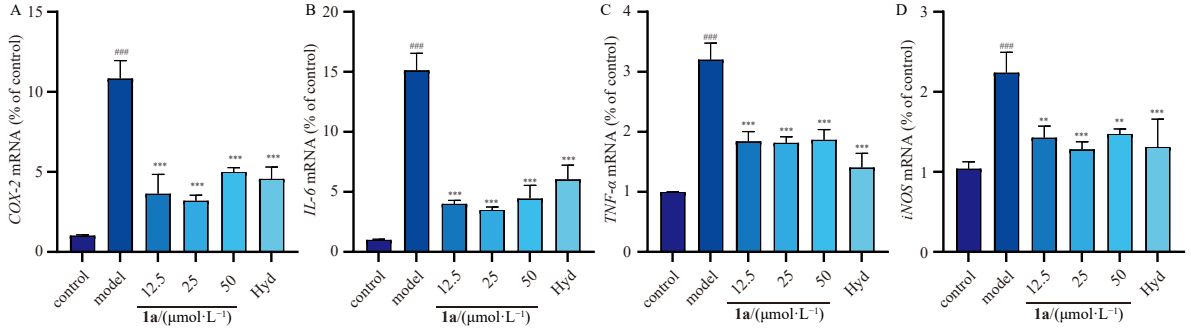

Fig. 5 The mRNA levels of *COX-2* (A), *IL-6* (B), *TNF-α* (C), and *iNOS* (D) genes were determined by real-time PCR. Data are presented means ± SD (n = 3). $^{###}P < 0.001$ *vs* control; $^{*}P < 0.05$, $^{**}P < 0.01$, $^{***}P < 0.001$ *vs* LPS.

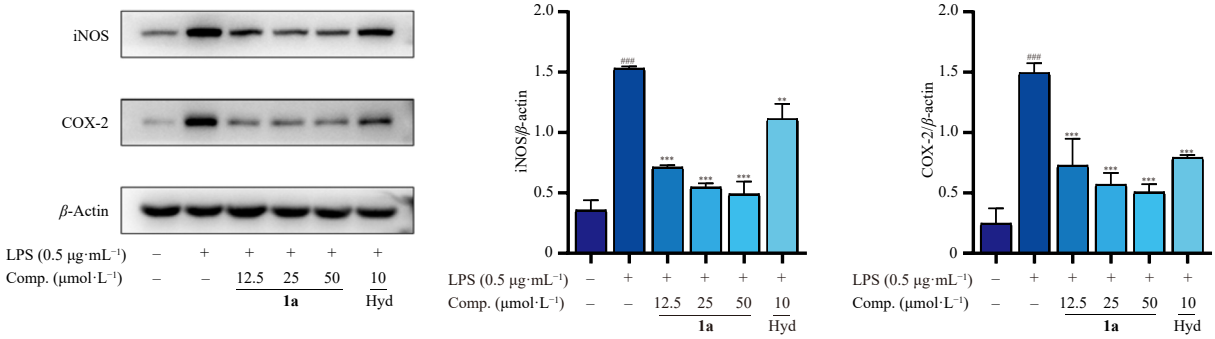

Fig. 6 Impact of **1a** on the protein expression levels of iNOS and COX-2 in LPS-stimulated BV-2 cells. Data represent means ± SD (n = 3). $^{###}P < 0.001$ *vs* control; $^{*}P < 0.05$, $^{**}P < 0.01$, $^{***}P < 0.001$ *vs* LPS.

erythro may be greater than *threo*; and (7*S*,8*S*) may be better than (7*R*,8*R*) lignin. Furthermore, comparison of the anti-inflammatory activities of two pairs of enantiomers (**3a**/**3b** and **5a**/**5b**) indicated that the absolute configuration might play a significant role in their inhibitory activity against NO production.

3. Experimental

3.1. General experimental procedures

Optical rotations were obtained with a JASCO P1020 polarimeter (JASCO) P1020 polarimeter (JASCO, Japan) at room temperature (RT). UV spectra were measured with a JASCO V550 (JASCO, Japan) instrument. IR spectra were acquired using a JASCO FT/IR-480 plus spectrometer (KBr) (JASCO, Japan). NMR spectra were obtained on Bruker AV-400 or AV-600 MHz NMR spectrometers (Bruker, Switzerland) with solvent signals ($CDCl_3$: δ_H 7.26/δ_C 77.16; CD_3OD: δ_H 4.87/δ_C 49.00) as an internal reference. HR-ESI-MS spectra were obtained using a Waters Synapt G2 mass spectrometer (Waters, USA). Analytical HPLC (Shimadzu, Japan) was conducted on a Shimadzu HPLC system with an LC-20AB solvent delivery system and an SPD-20A UV/vis detector using Phenomenex Gemini C_{18} column (5 μm, 4.6 mm × 250 mm, Phenomenex Gemini, USA), Zhongpu Science Polo-RP column (5 μm, Φ 4.6 mm × 250 mm; Zhongpu Inc., Fujian, China) and EnantioPak OD column (5 μm, Φ 4.6 mm × 250 mm; Research & Creativity Biotechnology Co., Ltd., Guangzhou, China). Semipreparative HPLC (Shimadzu, Japan) was performed on a Shimadzu LC-6AD liquid chromatography system equipped with an SPD-20A detector on a Phenomenex Gemini C_{18} column (5 μm, 10 mm × 250 mm). Preparative HPLC was conducted on a Phenomenex Gemini C_{18} column (5 μm, 20 mm × 250 mm) under comparable chromatographic conditions. Diaion HP-20 (Mitsubishi Chemical Co., Japan), silica gel (100–200 and 200–300 mesh, Qingdao Marine Chemical Co., China), MCI gel CHP20P (75–150 μm, Mitsubishi Chemical Co., Japan), Sephadex LH-20 (GE Healthcare, Britain), and octadecyl silane (ODS) silica gel (12 nm, S-50 μm, YMC, Britain) were used for column chromatography (CC). Precoated silica gel GF_{254} plates (China) for thin-layer chromatography (TLC) were bought from Qingdao Marine Chemical Co. (Qingdao, China). All analytical grade reagents (China) were from Concord Chemicals Co., Ltd. (China).

3.2. Plant material

The leaves of *I. dunnianum* were purchased from the Chinese Medicine Market in Ji'an County in September 2018, which were identified by Prof. Zhou Wu (Jiangsu Kanion Pharmaceutical Co., Ltd., Lianyungang, China). A sample (2018ID101) was deposited in the Institute of Traditional Chinese Medicine & Natural Products, College of Pharmacy, Jinan University, Guangzhou, China.

3.3. Extraction and isolation

The air-dried leaves of *I. dunnianum* (ID, 15.5 kg) were extracted with 50% EtOH through heat reflux three times (2 h each). The total extracts (IDEs, 2 kg) were obtained through evaporation under reduced pressure. IDEs were fractionated by HP-20 CC (ϕ 14 cm × 140 cm) and eluted with EtOH–H_2O [0∶100, 30∶70, 50∶50, 95∶5 (*V*/*V*)] gradient to yield 4 fractions [ID-1 (1278 g), ID-2 (280 g), ID-3 (204 g), ID-4 (95 g)]. Fr. ID-2 (280 g) underwent separation over a silica gel column (200–300 mesh, 3.0 kg, ϕ 12 cm × 75 cm) eluting with a CH_2Cl_2–CH_3OH gradient [100∶0, 95∶5, 90∶10, 85∶15, 80∶20, 70∶30, 60∶40, 0∶100 (*V*/*V*)] to produce 6 fractions [Frs. 2A–2F]. Fr. 2D (65.0 g, 23.2%) was subjected to ODS CC (600 g, ϕ 7 cm × 75 cm) using a CH_3OH–H_2O gradient elution [10∶90–60∶40, 100∶0 (*V*/*V*)] to generate 9 fractions [Frs. 2D1–2D9]. Fr. 2D4 (15.7 g, 24.2%) and 2D7 (4.8 g, 7.4%) were further separated by TOYOPEARL HW-40C column (200 g, ϕ 4 cm × 45 cm) eluting with CH_3OH–H_2O [20∶80 (*V*/*V*)]

to yield 6 fractions [Frs. 2D4A–2D4F] and 5 fractions [Frs. 2D7A–Fr. 2DE], respectively. Fr. 2D4D (4.5 g, 28.7%) underwent chromatography by Sephadex LH-20 (50 g, ϕ 2 cm × 140 cm) eluting with CH_3OH–H_2O [50∶50 (*V*/*V*)] to produce 3 subfractions [Frs. 2D4D1–2D4D3]. Fr. 2D4D3 (4.1 g) was purified using preparative HPLC [20% CH_3CN–H_2O, 8 mL·min^{-1}] to afford compounds **6** (9.6 mg, t_R 8.9 min), **7** (4.4 mg, t_R 13.6 min), **11** (85.7 mg, t_R 16.1 min) and **12** (44.3 mg, t_R 17.6 min). Fr. 2D7E (1.2 g) was isolated using semipreparative HPLC [40% CH_3OH–H_2O), 3 mL min^{-1}] to yield **8** (4.4 mg, t_R 14.1 min), **9** (71.8 mg, t_R 16.3 min) and **10** (1.3 mg t_R 17.5 min).

Fr. ID-4 (92 g) was separated over a silica gel column eluting with a cyclohexane–EtOAc gradient (100∶0, 98∶2, 95∶5, 90∶10, 85∶15, 80∶20, 70∶30, 60∶40, 50∶50, 0∶100) to afford 10 fractions (Frs. 4A to 4L). Fr. 4E (3.8 g) and 4F (5.2 g) were chromatographed by ODS CC using a CH_3OH–H_2O gradient elution (30∶70–70∶30, 100∶0) to give 3 fractions (Frs. 4E1–4E3) and 7 fractions (Frs. 4F1–4F7), respectively. Fr. 4E3 (0.8 g), 4E4 (0.5 g) and 4F5 (0.4 g) were separated using semipreparative HPLC to yield **1** (10.1 mg, t_R 9.6 min, 45% CH_3CN–H_2O, 3 mL·min^{-1}), **2** (2.3 mg, t_R 11.3 min, 45% CH_3CN–H_2O, 3 mL·min^{-1}), **3** (30.1 mg, t_R 8.9 min, 55% CH_3CN–H_2O, 3 mL·min^{-1}), **4** (3.5 mg, t_R 12.6 min, 60% CH_3CN–H_2O, 3 mL·min^{-1}) and **5** (6.3 mg, t_R 13.2 min, 55% CH_3CN–H_2O, 3 mL·min^{-1}). Compound **3** was further isolated by semipreparative chiral HPLC (EnantinPak OJ-3, 5 μm, 250 × 4.60 mm, 62% CH_3CN–H_2O (0.1% HCOOH), 1 mL·min^{-1}) to get **3a** (7.8 mg, t_R 14.0 min) and **3b** (10.6 mg, t_R 17.0 min). **1**, **2**, **4** and **5** were further isolated by semipreparative chiral HPLC (EnantinPak OD, 5 μm, 250 × 4.60 mm, 60% CH_3CN–H_2O (0.1% HCOOH), 1 mL·min^{-1}) to get **1a** (1.6 mg, t_R 19.0 min), **1b** (2.3 mg, t_R 23 min), **2a** (0.2 mg, t_R 19.5 min), **2b** (0.3 mg, t_R 22.0 min), **4a** (1.5 mg, t_R 19.0 min), **4b** (1.4 mg, t_R 21.5 min), **5a** (1.9 mg, t_R 12.0 min), and **5b** (1.8 mg, t_R 13.0 min).

3.4. Identification of new compounds

(–)-(7*S*,8*S*)-morinol M/(+)-(7*R*,8*R*)-morinol M (**1a**/**1b**): colorless oil. **1a**: $[\alpha]_D^{25}$ −35.47 (*c* 0.50, MeOH); **1b**: $[\alpha]_D^{25}$ +39.24 (*c* 0.49, MeOH). HR-ESI-MS (positive) *m/z* 313.1829 $[M + H]^+$ (Calcd. for $C_{20}H_{25}O_3^+$, 313.1804); UV (MeOH) λ_{max} (log ε): 202 (4.06), 228 (3.69), 260 (3.93) nm; IR (KBr) ν_{max} 3332, 2941, 2833, 1609, 1511, 1457, 1246, 1175, 1112, 1021, 835, 537 cm^{-1}; ^{1}H and ^{13}C NMR spectroscopic data (Table 1).

(–)-(7*S*,8*R*)-morinol N/(+)-(7*R*,8*S*)-morinol N (**2a**/**2b**): colorless oil. **2a**: $[\alpha]_D^{25}$ −25.54 (*c* 0.47, MeOH); **2b**: $[\alpha]_D^{25}$ +27.83 (*c* 0.50, MeOH). HR-ESI-MS (positive) *m/z* 313.1839 $[M + H]^+$ (Calcd. for $C_{20}H_{25}O_3^+$, 313.1804); UV (MeOH) λ_{max} (log ε): 202 (4.06), 228 (3.69), 260 (3.93) nm; IR (KBr) ν_{max} 3332, 2941, 2833, 1609, 1511, 1457, 1246, 1175, 1112, 1021, 835, 537 cm^{-1}; ^{1}H and ^{13}C NMR spectroscopic data (Table 1).

(+)-(7*S*,8*S*,7′*S*,7″*S*)-anemonenorin A/(–)-(7*R*,8*R*,7′*R*,7″*R*)-anemonenorin A (**3a**/**3b**): colorless oil. **3a**: $[\alpha]_D^{25}$ +42.38 (*c* 0.50, MeOH); **3b**: $[\alpha]_D^{25}$ −48.99 (*c* 0.50, MeOH). HR-ESI-MS (positive) *m/z* 443.1833 $[M + Na]^+$ (Calcd. for $C_{26}H_{28}O_5Na^+$, 443.1834); UV (MeOH) λ_{max} (log ε): 202 (4.22), 225 (4.00), 260 (4.04) nm; IR (KBr) ν_{max} 3338, 2935, 2835, 1613, 1513, 1461, 1400, 1303, 1246, 1175, 1128, 1079, 1024 cm^{-1}; ^{1}H and ^{13}C NMR spectroscopic data (Table 1).

(–)-(7*R*,8*R*,7′*R*,9″*R*)-illiciumione A/(+)-(7*S*,8*S*,7′*S*,9″*S*)-illiciumione A (**4a**/**4b**): colorless oil. **4a**: $[\alpha]_D^{25}$ −59.82 (*c* 0.50, MeOH); **4b**: $[\alpha]_D^{25}$ +61.46 (*c* 0.45, MeOH). HR-ESI-MS (positive) *m/z* 469.1983 $[M + Na]^+$ (Calcd. for $C_{28}H_{30}O_5Na^+$, 469.1991); UV (MeOH) λ_{max} (log ε): 202 (4.24), 225 (4.03), 260 (4.07) nm; IR (KBr) ν_{max} 3318, 2940, 2833, 1609, 1512, 1454, 1303, 1247, 1176, 1128, 1021, 827, 566 cm^{-1}; ^{1}H and ^{13}C NMR spectroscopic data (Table 1).

(+)-(7*R*,8*R*,7′*R*,8′*S*)-verimol H/(–)-(7*S*,8*S*,7′*S*,8′*R*)-verimol H (**5a**/**5b**): colorless oil. **5a**: $[\alpha]_D^{25}$ +37.41 (*c* 0.51, MeOH); **5b**: $[\alpha]_D^{25}$ −38.14 (*c* 0.55, MeOH). HR-ESI-MS (positive) *m/z* 351.1573 $[M + Na]^+$ (Calcd. for $C_{20}H_{24}O_4Na^+$, 351.1572); UV (MeOH) λ_{max} (log ε): 202 (4.11), 225 (3.90), 260 (3.94) nm; IR (KBr) ν_{max} 3316, 2945, 2832, 1654, 1449, 1115, 1018 cm^{-1}; ^{1}H and ^{13}C NMR spectroscopic data (Table 1).

3.5. ECD calculation

The experimental details are described in the Supporting information (SI–S1).

3.6. Anti-inflammatory activities assays

The experimental details are described in the Supporting information (SI–S2).

Funding

This work was supported by the Basic Research Program of the Natural Science Fund-Frontier Leading Technology Basic Research Special Project (No. SBK2023050003) and by the University Science and Technology Innovation Team of Department of Education of Guizhou Province (No. QJJ[2023]099).

Supporting information

HR-ESI-MS and 1D and 2D NMR spectra of compounds **1a**/**1b**–**5a**/**5b** can be requested by sending E-mail to the corresponding authors.

Declaration of competing interest

These authors have no conflict of interest to declare.

References

1 WFO. *Illicium dunnianum* Tutcher. 2003. http://www.worldfloraonline.org/taxon/wfo 0001219855
2 Wu Z. *Flora of China*. Beijing: Science Press. 1978:321-329.
3 Lin Q. Medicinal plant resources of *Illicium L. Chin Tradit Herb Drugs*. 2002; 33(7):81-84.
4 Deng HP, Sun L, Xi ZX, et al. Progress on chemical and pharmacological research of C6-C3 compounds in genus *Illicium*. *J Pharm Pract*. 2012;30(1):8-13. https://doi.org/10.3969/j.issn.006-0111.2012.01.003.
5 Bai J, Chen H, Fang ZF, et al. Sesquiterpenes and neolignans from the roots of *Illicium dunnianum*. *J Asian Nat Prod Res*. 2012;14(10):940-949. https://doi.org/10.1080/10286020.2012.729507.
6 Li J, Geng D, Xu J, et al. Antidepressant-like effect of macranthol isolated from *Illicium dunnianum* tutch in mice. *Eur J Pharmacol*. 2013;707(3):112-119. https://doi.org/10.1016/j.ejphar.2013.03.010.
7 Geng D, Weng LJ, Han YY, et al. Chemical constituents from *Illicium dunnianum*. *Adv Mater Res*. 2012;550-553:1586-1589. https://doi.org/10.4028/www.scientific.net/AMR.550-553.1586.
8 Geng D, Weng LJ, Han YY, et al. Flavonoids from *Illicium dunnianum*. *Adv Mater Res*. 2012;610-613:3375-3377. https://doi.org/10.4028/www.scientific.net/AMR.610-613.3375.
9 Bai J, Chen H, Fang ZF, et al. Sesquiterpenes from the roots of *Illicium dunnianum*. *Phytochemistry*. 2012;80:137-147. https://doi.org/10.1016/j.phytochem.2012.05.015.
10 Zhang JW. Chemical constituents of the stems and leaves of *Illicium dunnianum* Tutch. *Chin Tradit Herb Drugs*. 1989;14(1):36-37.
11 Zhang LF, Lin KZ, Yang WD, et al. Identification of the original plant and miscible products of *Illicium dunnianum*. *Chin J Tradit Chin Med*. 1995;20(12): 717-718.
12 Zeng WL, Song JL, Ceng YF, et al. Effect of alcohol extract of *Illicium dunnianum* on immune function in mice. *J Guiyang Univ Tradit Chin Med*. 1992;14(2):60-62.
13 Luo L, Liu XL, Li J, et al. Macranthol promotes hippocampal neuronal proliferation in mice *via* BDNF-TrkB-PI3K/Akt signaling pathway. *Eur J Pharmacol*. 2015;762:357-363. https://doi.org/10.1016/j.ejphar.2015.05.036.
14 Ma SJ, Li HB, Li T, et al. Illiciumlignans G–O from the leaves of *Illicium dunnianum* and their anti-inffammatory activities. *RSC Adv*. 2021;11(49): 30725-30733. https://doi.org/10.1039/D1RA03520G.
15 Li HB, Ma SJ, Shan YX, et al. Eight new phenolic acids from the leaves of *Illicium dunnianum* and their osteoprotective activities. *RSC Adv*. 2022; 12(33):21655-21661. https://doi.org/10.1039/D2RA03589H.

16 Shao JR, Ma SJ, Li T, et al. Two new chemical constituents from the leaves of *Illicium dunnianum*. *Nat Prod Res*. 2023;37(8):1233-1240. https://doi.org/10.1080/14786419.2021.2004599.
17 He XQ, Li HB, Li T, et al. One undescribed glycoside benzofuran derivative and a new *p*-hydroxybenzoate glycoside from the leaves of *Illicium dunnianum* Tutcher. *Nat Prod Res*. 2024;38(18):3130-3139. https://doi.org/10.1080/14786419.2023. 2216348.
18 Su B, Takaishi Y, Kusumi T. Morinols A–L, twelve novel sesquineolignans and neolignans with a new carbon skeleton from *Morina chinensis*. *Tetrahedron*. 1999;55(51):14571-14586. https://doi.org/10.1016/S0040-4020(99)00933-3.
19 Mou L, Wei M, Wu H, et al. Structure elucidation of two new norlignans from *Anemone vitifolia* and their anti-inflammatory activities. *Chem Biodivers*. 2020;17(7):e2000184. https://doi.org/10.1002/cbdv.202000184.
20 Trung TN, Thi TL, Thi XD, et al. Amenyunnaosides A–C, three new neolignans isolated from *Amentotaxus yunnanensis* and their anti-inflammatory activities. *Chem Biodivers*. 2023;20(6):e202300604. https://doi.org/10.1002/cbdv.202300604.
21 Yen DTH, Hang DTT, Yen PH, et al. Four undescribed compounds isolated from the aerial parts of *Phyllanthus cochinchinensis* with antimicrobial activity and NO production inhibitory activity in LPS activated RAW 264.7 cells. *Chem Biodivers*. 2024;21(3):e202302105. https://doi.org/10.1002/cbdv.202302105.
22 Li W, Wu Z, Xia Y, et al. Antiviral and antioxidant components from the fruits of *Illicium verum* Hook. f. (Chinese Star Anise). *J Agric Food Chem*. 2022;70(12):3697-3707. https://doi.org/10.1021/acs.jafc.1c08376.
23 Sy L, Brown G. Novel phenylpropanoids and lignans from *Illicium verum*. *J Nat Prod*. 1998;61(8):987-992. https://doi.org/10.1021/np9800553.
24 Takara K, Matsui D, Wada K, et al. New phenolic compounds from Kokuto, noncentrifuged cane sugar. *Biosci Biotech Bioch*. 2003;67(2):376-379. https://doi.org/10.1271/bbb.67.376.
25 Kuang H, Xia Y, Yang B, et al. Lignan constituents from *Chloranthus japonicus* Sieb. *Arch Pharm Res*. 2009;32:329-334. https://doi.org/10.1007/s12272-009-1303-1.
26 Takeda Y, Mima C, Masuda T, et al. Glochidioboside, a glucoside of (7*S*,8*R*)-dihydrodehydrodiconiferyl alcohol from leaves of *Glochidion obovatum*. *Phytochemistry*. 1998;49(7):2137-2139. https://doi.org/10.1016/S0031-9422(98)00362-8.
27 Zhang Y, Liu Y, Li Y, et al. Phenolic constituents from the roots of *Alangium chinense*. *Chin Chem Lett*. 2017;28(1):32-36. https://doi.org/10.1016/j.cclet.2016.05.012.
28 Tang W, Liu Y, Yu S, et al. New sesquiterpene lactone and neolignan glycosides with antioxidant and anti-inflammatory activities from the fruits of *Illicium oligandrum*. *Planta Med*. 2007;73(5):484-490. https://doi.org/10.1055/s-2007-967189.
29 He Z, Ma C, Tan G, et al. Rourinoside and rouremin, antimalarial constituents from *Rourea minor*. *Phytochemistry*. 2006;67(13):1378-1384. https://doi.org/10.1016/j.phytochem.2006.04.012.